Agricultural Load Modeling Based on Crop Evapotranspiration and Light Integration for Economic Operation of Greenhouse Power Systems

Zeming Li, Junyong Liu, *Member, IEEE*, Yue Xiang, *Senior Member, IEEE*, Xin Zhang, *Senior Member, IEEE*, and Yanxin Chai

***Abstract*—The threat of environmental degradation attracts great attention to clean energy production and transportation. However, the limited scope of energy consumption causes the large-scale of clean energy sources to be abandoned in Sichuan province. In the meantime, the development of modern greenhouse cultivation has transformed the agriculture industry to develop a brand-new type of electrical load in the grid. Consequently, the agricultural load can be used to consume the clean energy while facilitating plant growth. In this paper, an innovative agricultural load model is proposed based on crop evapotranspiration and daily light integration. Furthermore, the proposed agricultural load model is also applied to investigate the electricity consumption of five types of crop planting. The results illustrate that the power consumption is primarily driven by an artificial lighting compensation system.**

***Index Terms*—Agriculture load model, crop evapotranspiration model, daily light integration model, power consumption.**

I. Introduction

SINCE the beginning of the 21st century, the world's science, technology and living standards have continued to develop rapidly, which has led to significant population growth and urban area expansion. The increased life requirements have brought enormous pressure on the earth's limited resources, including food, water, energy, land and ecosystems [1]. A food-water-energy (FWE) nexus approach has been proposed as a main research topic and global concern in recent years [2]. Moreover, climate change, land deforestation desertification, and salinization have caused instable yields of agricultural production with increasing concerns about food security [3]. To solve this issue, greenhouse "protected cultivation" can form a relatively stable microclimate that is not affected by the external environment, making agricultural production feasible for all seasons without geographical constraints. In addition, the greenhouse's climate control and automation equipment consume electricity at various planting stage with temporal effect. As a result, agricultural production urgently requires sufficient energy supply. Hence, agricultural load has become an important type of load in the power grid.

In recent years, with the development of clean energy generation, the power market in Sichuan has presented a critical situation of oversupply, especially with large-scale redundancy of hydropower. Consequently, a massive amount of water sources have been abandoned every year. Hence, under the background of the national power market reform, how to properly consume the surplus hydropower has become the key issue restricting the development of the Sichuan power market. Liu *et al*. [4] intensively analyzed the current problems of the power grid with agricultural load, and the potential of using agricultural load to consume the clean energy. It has been noted that agricultural load modeling is one of the primary difficulties that drives the success of power and agricultural system integration. In the past, load modeling methods are primarily grouped into two categories: a component-based modeling approach and measurement-based modeling approach. Based on a component-based approach, an equivalent thermal parameter model of the central air-conditioning system in public buildings considering the thermodynamic characteristics was presented in [5]. Quilumba *et al*. [6] established a ZIP based household load model considering the utilization of televisions. Considering the time features of load demand, a bottom-up time-variant load model was proposed in [7]. Wang *et al*. [8] employed a wavelet analysis and clustering method to preprocess and classify the load signal, which improved the accuracy of the parameter identification of the load modeling. Moreover, a measurement-based composite load model was proposed in [9], while a questionnaire-based method was used in [10] for selecting proper load models.

At present, the agricultural load modeling is primarily identified by the measurement-based method, i.e., using the measured data to identify the structure and parameters of the load model. Based on data measurement, a rural power system load model was proposed by using regression analysis [11]. The agricultural load in Heilongjiang province of China was

Manuscript received April 4, 2019; revised July 19, 2019; accepted September 19, 2019. Date of online publication October 7, 2019; date of current version July 31, 2020. This work was supported by the Talents' Training Quality and Teaching Reform Project for 2018-2020 Higher Education in Sichuan Province (JG2018-10) and the New Century Higher Education Teaching Reform Project of Sichuan University under Grant No. SCU8007.

Z. M. Li, J. Y. Liu, Y. Xiang (corresponding author, e-mail: xiang@scu.edu.cn; ORCID: https://orcid.org/0000-0001-8456-1195), and Y. X. Chai are with the College of Electrical Engineering, Sichuan University, Chengdu 610065, China.

X. Zhang is with Energy and Power Theme, School of Water, Energy and Environment, Cranfield University, Cranfield MK43 0AL, UK.

DOI: 10.17775/CSEEJPES.2019.00750

developed based on a neural network with agricultural related power data, which provided a reference for future agricultural development [12]. However, these load models are based on specific data collection from the local system. Therefore, the model only can be applied in specific areas. In addition, the model is a data-driven empirical approach which could not deal with microscopic simulation and mechanism analysis of agricultural load characteristics. Furthermore, these models are lacking of key factors that fundamentally drive the energy consumption in an agriculture system, which could not provide any contribution to manage and optimize the agricultural power load, nor to analyze the agricultural load impact on rural distribution network planning. Under this circumstance, based on the crop evapotranspiration and daily light integration modeling, an agricultural load model is established in this paper to optimize and evaluate the electricity consumption and efficiency improvement of five different crops growth in a solar greenhouse.

II. Modeling of Crop Growth with Environmental Factors

The solar greenhouse constructs a suitable environment for crop growth with required soil, water, and climate resources to increase plant productivity and quality, with opportunities to enhance market supply for all seasons. In the greenhouse environment, there are many coupled environmental factors that influences the crop growth, primarily soil moisture, illumination, temperature, carbon dioxide concentration, and humidity, which make the greenhouse a complex system. In this paper, illumination and soil moisture, which are correlated to the electricity supply, are analyzed and discussed.

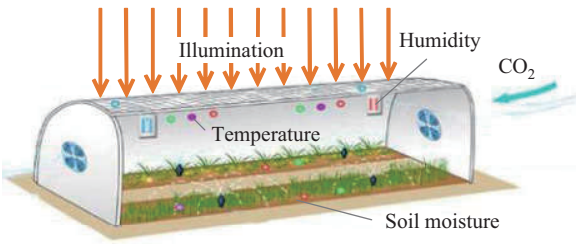

Fig. 1. Environmental factors to impact plant growth in the greenhouse.

A. Illumination

As the major energy source of the greenhouse ecosystem, sunlight is the vital nature source for the photosynthesis process of plants. The crop uses the photosynthetic pigments in the body to capture the energy from sunlight to meet the energy requirements of various life activities. Sufficient sunlight ensures organic matter accumulation in the crop itself, promoting crop growth and increasing the dry weight of the crops. Furthermore, lighting also effectively controls the various life activities in plants, such as the photoperiod of plants which induces crop flowering, dormancy and vegetative growth [13], [14]. Moreover, the illumination quality of the light source can promote the compounding of various pigments in the body of the crop, improve the quality of the crops, and increase the market competitiveness and value of the crops [15].

In order to evaluate the quantity of power required in the illumination system, it is necessary to know the light required for crop growth. There are many ways to measure the light intensity of various light sources, such as foot-candles, lux, lumens, etc. However, none of these methods are commonly accepted in the field of agriculture. At present, the daily light integral (DLI) recommended by the American Horticultural Society is commonly used to describe photosynthetically active radiation (PAR) associated with the photosynthesis process of plant growth, measured by mol/(m^2· d) [16]. The mathematical representation is shown as follows [17]:

$$D = L_{\text{intensity}} \cdot L_{\text{cycle}} \cdot 3600/10^6 \tag{1}$$

where D is the daily light integral, $L_{\text{intensity}}$ is the light intensity, and L_{cycle} is the time period.

The plants can be typically categorized into five types, which are very low light (less than 5 mol/(m^2·d)), low light (5–10 mol/(m^2·d)), moderate light (10–20 mol/(m^2·d)), high light (20–30 mol/(m^2·d)), and very high light (30–60 mol/m^2/d). According to the required DLI for each type of plant which is appropriate to its growth [18], a DLI between 4 to 12 mol/(m^2·d) is the typical range for plant growth and development [19]. However, due to the variation in latitude, cloud cover and haze density, direct sunlight has a reduced effect on plant growth. Consequently, it is often difficult to achieve the optimal lighting environment for plant growth in the nature environment. Therefore, artificial lighting compensation has become an effective solution to improve the plant illumination environment, and reduce the crop growth cycle [20].

In the meantime, the light absorption ability of plants is limited. When the light is too strong, the large amount of solar energy accumulated on the leaves will cause the plant's surface temperature to increase at a high level and burn the leaves. This would reduce the photosynthetic rate of the plants and adversely affect their growth which is called a light saturation phenomenon.Therefore, the plant light saturation point can be used as the most suitable light intensity, and becomes the target DLI to maximize daily plant growth with no energy waste. Due to climate and environmental factors, when natural light cannot meet the amount of light required for plant growth, the artificial light compensates for the light shortage, which is represented as:

$$D_{\text{compensation}} = D_{\text{target}} - D_{\text{sunlight}} \tag{2}$$

where D_{sunlight} is the amount of natural sunlight, which can be derived by professional equipment. $D_{\text{compensation}}$ is the light compensation from artificial sources, and D_{target} is the target light that can be calculated by (3), with the *LSP* (light saturation point) indicating the point of light saturation [18].

$$D_{\text{target}} = L_{\text{LSP}} \times 0.0432 \tag{3}$$

where L_{LSP} represents the average of 70% maximum photosynthesis.

Currently, the LED light is widely used in a greenhouse artificial lighting compensation system [21]. The electricity

consumption of an artificial lighting system can be described as a function of the required compensation light amount, the power output of LED and the light illumination per unit power, as shown:

$$P_{\text{light}} = \iint \frac{D(x,y)}{D_{\text{light}}} \cdot P_{\text{LED}}(x,y)\mathrm{d}x\mathrm{d}y \tag{4}$$

where $D(x,y)$ represents the distribution of DLI required for crop growth within the greenhouse, which is equal to $D_{\text{compensation}}$ in each time period; D_{light} is the amount of DLI emitted by the unit power of the LED, and $P_{\text{LED}}(x,y)$ illustrates that the distribution of LED load in the greenhouse.

B. Soil Moisture

Freshwater is an important component containing in the plant body, which plays an important role in the various life activities of plants. An irrigation system is commonly used in a greenhouse to supply water and maintain soil moisture for the plants. To establish the load model of the irrigation system, the crop daily water requirement for growth is measured.

The plant water requirement primarily consists of transpiration (T), evaporation (E) and the water that constitutes the plant's body. Since the water retained in the plant is only a small proportion compared with the water lost through evaporation, the water in the plant will be ignored when estimating the water requirement. The combination of two separate processes, whereby water is lost on the one hand from the soil surface by evaporation, and on the other hand from the crop by transpiration, is referred to as evapotranspiration (ET) [22].

The evapotranspiration of crops can be directly derived by using instrument measurement or experience formulas. However, such expensive measurement or empirical formulas are not satisfied by theoretical analysis. So, the Penman-Monteith model [23] is utilized to precisely calculate evapotranspiration, which is based on the energy balance theory and turbulent diffusion theory (the energy flow in farmland is shown in Fig. 2).

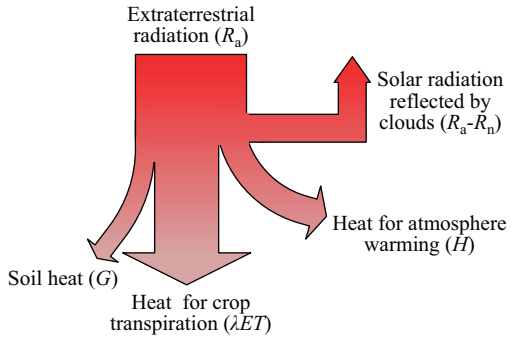

Fig. 2. Solar radiation energy transfer map in a farmland, whereby the energy balance is described as: $R_n = \lambda ET + H + G$.

However, the parameters of surface resistance and aerodynamic resistance are too complicated to calculate in the model [24], which makes it an impractical application for the model. Therefore, this paper adopts the widely applied dual crop coefficient model [25]–[29] which is modified from the Penman-Monteith model by the Food and Agriculture Organization of the United Nations (FAO) to calculate the crop evapotranspiration as shown in (5), and the parameters in this model are discussed below.

$$\begin{aligned} ET_0 = ET_{\text{rad}} + ET_{\text{aero}} &= \frac{0.408\Delta(R_n - G)}{\Delta + \gamma(1 + 0.34U_2)} \\ &+ \frac{\gamma \cdot 900 \cdot U_2(e_s - e_a)}{(\Delta + \gamma(1 + 0.34U_2)) \cdot (T + 273)} \\ ET_c = K_c \times ET_0 &= (K_s K_{cb} + K_e) ET_0 \end{aligned} \tag{5}$$

where ET_{aero} and ET_{rad} represent radiation terms of crop evapotranspiration and aerodynamic terms of crop evapotranspiration respectively. R_n represents solar radiation. G represents the soil heat flux. e_s and e_a represent saturated vapor pressure and ambient vapor pressure respectively. γ represents the psychrometric constant. Δ, U_2 represent the slope of the saturated vapor pressure curve and the wind speed at 2 m above the ground surface, respectively. T represents average air temperature. ET_c, defined as the crop evapotranspiration under standard conditions, is the evapotranspiration from disease-free, well-fertilized crops, grown in large fields, under optimum soil water conditions, and achieving full production under the given climatic conditions. ET_0 is called the reference crop evapotranspiration. K_c represents the crop coefficient, which scales the reference evapotranspiration to explain specific effects of crops on evapotranspiration and variations in different crop growing seasons. K_{cb} is the basal crop transpiration coefficient, K_s is the waterstress coefficient (0–1) that shows the plant water status, and K_e is the evaporation coefficient. The value of K_{cb} under standard climatic conditions (daily minimum relative humidity $RH_{\min} = 45\%$ and wind speed at 2 m $U_2 = 2$ m/s) is available through the basic crop coefficient table provided by FAO, and can be corrected using (6) for non-standard climatic conditions.

$$K_{cb} = K_{cb} + [0.04(U_2 - 2) - 0.004(RH_{\min} - 45)] \left(\frac{h}{3}\right)^{0.3} \tag{6}$$

The solar radiation R_n in (5) is corresponding to the differences between the incoming short-wave radiation R_{ns} and the outgoing long-wave radiation R_{nl}, derived by (7).

$$\begin{aligned} R_n &= R_{ns} - R_{nl} \\ &= 28.952 d_r (0.25 + 0.5n/N)(W_s \sin(\varphi)\sin(\delta) \\ &\quad + \sin(W_s)\cos(\varphi)\cos(\delta)) - 2.45 \times 10^{-9}(0.9n/N \\ &\quad + 0.1)(0.34 - 0.14\sqrt{e_a})(T_{kx}^4 + T_{kn}^4) \end{aligned} \tag{7}$$

where d_r and δ are the inverse relative distance from Earth-Sun and the solar declination respectively. Those are functions of the Julian day number J, given as (8) and (9), and W_s represents the sunset hour angle, which is obtained by (10). T_{kx} is maximum absolute temperature and T_{kn} is minimum absolute temperature. e_a is the ambient vapor pressure. n represents the actual duration of sunshine. N represents the maximum possible duration of sunshine or daylight hours, and φ is latitude.

$$\delta = 0.409 \sin(0.0172J - 1.39) \tag{8}$$

$$d_{\mathrm{r}} = 1 + 0.033\cos(0.0172J) \tag{9}$$

$$W_{\mathrm{s}} = \arccos(-\tan\phi \cdot \tan\delta) \tag{10}$$

Saturated vapor pressure e_{s} and ambient vapor pressure e_{a} in (5), are calculated by (11). In particular, when the relative saturation humidity $RH = 100$, the ambient vapor pressure becomes e_{s}.

$$e_{\mathrm{a}} = 0.611\exp\left(\frac{17.27T}{T+237.3}\right)\cdot\frac{RH}{100} \tag{11}$$

Soil heat flux G in (5), can be simplified by the temperature difference shown as (12), where T_d and T_{d-1} are the temperatures of intra-day d and previous day $d-1$, respectively.

$$G = 0.38(T_d - T_{d-1}) \tag{12}$$

The psychrometric constant γ in (5), can be derived by (13).

$$\gamma = \frac{\mathrm{C_p}P}{\varepsilon\lambda}\times 10^{-6} \tag{13}$$

where C_{p} is the specific heat of the humid atmosphere, taking 1.013 KJkg^{-1}°C^{-1}, ε represents the ratio molecular weight of water vapour/dry air, taking 0.622 [30]. The atmospheric pressure P is a function of altitude, and λ represents the latent heat of vaporization, which is a function of temperature.

The slope of the saturated vapor pressure curve Δ in (5) can be obtained from (14).

$$\Delta = \frac{4098e_{\mathrm{a}}}{(T+237.3)^2} \tag{14}$$

Once the daily water demand of the plant is modeled, it is necessary to link between the water demand and power demand, which is given in [31]. This equation models the electric load of the irrigation system:

$$P_{\text{irrigation}} = E_{\mathrm{h}}\times\left(\frac{100}{\eta}\right) = V\times H\times\left(\frac{\rho g}{3600}\right)\times\left(\frac{100}{\eta}\right) \tag{15}$$

where $P_{\text{irrigation}}$ is the power of the drip irrigation system, W. E_{h} is hydraulic energy, kW·h. V is the volume of water, is the amount of water required for irrigation by a drip irrigation system in each hour ($\mathrm{ET_c}$), m^3/h. H is the pumping head of water, m. g is standard gravity (9.8 m/s^2). η is motor-pump efficiency, %. ρ is density of water, 1000 kg/m^3.

III. Simulation of Agricultural Load Model in Greenhouse System

A power system is designed to simulate agricultural load of the greenhouse with energy storage and renewable power generation. The greenhouse's power is supplied by the grid and a photovoltaic (PV) power generation system. An energy storage system is applied to absorb excessive PV generation, and provide additional power to the greenhouse. For agricultural load modeling, the irrigation system and artificial lighting compensation system are primarily considered on the load side of the greenhouse. In order to simplify the complexity of the system, the temperature and humidity control with ventilation and cooling load modeling are not considered.

The grid is assumed to be an infinite bus power system that constantly maintains the power balance in order to meet demand. Three locations (Chengdu, Jinan, and Haikou) with five common crops (i.e., lettuce, cabbage, sweet pepper, cucumber, and tomato) are selected as agricultural samples for the simulation. The geographical, climate and crop parameters involved in the simulation are shown in Tables I and II.

TABLE I
The Geographical Information of Three Cities

Location	Latitude (°)	Altitude (m)	Actual duration of sunshine (h)
Chengdu	30.67	600	2.87
Haikou	20.03	14.1	3.75
Jinan	36.68	51.6	4.44

TABLE II
The Crop Parameters of Five Crops

Crop	K_{cb}	Target DLI
Lettuce	0.95	14.51
Cabbage	0.9	17.35
Tomato	1.1	28
Sweet pepper	1	15
Cucumber	0.95	17.5

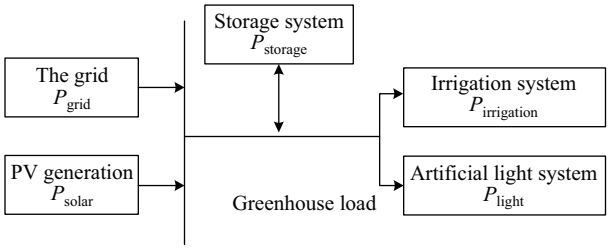

Fig. 3. Power system simulation with greenhouse load, PV generation and energy storage system.

To model the hourly agricultural load, the total daily amount of light compensation and water consumption are required to be satisfied, as shown in (16). Meanwhile, it is assumed that the irrigation and light compensation load can be timely adjusted in a day in accordance with the actual crop growth mechanism.

$$\sum_{i}^{n} ET_i = ET_{\mathrm{c}}, \sum_{i}^{n} D_i = D_{\text{compensation}} \tag{16}$$

where ET_i, D_i represent the amount of irrigation and light compensation for the period i. The water amount in each irrigation period needs to meet the constraints of existing irrigation regulations, which guarantees that the soil moisture is maintained in a range between soil water holding capacity (field capacity) and wilting point. The maximum light compensation at each time period is limited by the full power output of LED, as shown:

$$ET_i \in (D_{\mathrm{e\,min}}, D_{\mathrm{e\,max}}), D_i \in (0, D_{i\max}) \tag{17}$$

where $D_{\mathrm{e\,min}}$ and $D_{\mathrm{e\,max}}$ represent the minimum and maximum evaporation depth under the irrigation regulation. $D_{i\,\max}$ is the maximum DLI output.

In the design of an artificial light compensation system, excessive light energy would not be absorbed by plants, and further illumination would also have risks to burn the leaves. Thus, the light compensation system would be switched off

during the daytime when the natural sunlight is sufficient to save energy. To follow the actual crop growth law, the control logic for a light compensation system considering the photoperiod is shown as follows,

$$\begin{cases} XL_i = 0 & (i \in C \cup U) \\ XL_i = 1 & (i \in \bar{C} \cap \bar{U}) \end{cases} \tag{18}$$

where XL_i is a binary variable (0 or 1) indicating whether the light compensation system can be used in hour I over the whole day period. C represents the cycle of dark period still required for the necessary crop life activities, and U represents the time when the sunlight is sufficient.

The battery energy storage system (BESS) is set to store redundant PV generation, and discharge when the system generates insufficient power. Equation (19) describes the charging and discharging characteristics of the BESS:

$$\begin{aligned} &E_{\mathrm{B}}(t) = E_{\mathrm{B}}(t-1) + P_{\mathrm{BC}}(t) \cdot \eta_{\mathrm{c}} \cdot \Delta t - P_{\mathrm{Bd}}(t)/\eta_d \cdot \Delta t \\ &E_{B\,\min} < E_{\mathrm{B}}(t) \le E_{\mathrm{B}} \end{aligned} \tag{19}$$

where $E_{\mathrm{B}}(t)$ is the energy stored by the battery; η_{c} and η_d are the charging and discharging efficiency of the battery respectively; $E_{\mathrm{B}\,\min}$ is the minimum of the battery storage capacity; E_{B} is the rated energy storage capacity; and P_{BC}, P_{Bd} is the charge and discharge power.

The power balance equation of the whole system during the operation of greenhouse is as follows:

$$P_{\text{solar}} + P_{\text{grid}} = P_{\text{storage}} + P_{\text{light}} + P_{\text{irrigation}} \tag{20}$$

where P_{solar}, P_{grid}, P_{storage}, P_{light}, $P_{\text{irrigation}}$ are the power of the photovoltaic system, the purchased power of the external power grid, the charge-discharge power of the storage system, the load of artificial lighting compensation system, and the load of the irrigation system, respectively. Due to the fluctuation of the supply and demand within the grid, the electricity price is not constant within a day, which has a peak-to-valley price difference. Considering the economic operation of the green house with agricultural load, the optimization objective is to minimize the total cost of power purchased from the external grid when operating in the day-ahead optimization design, which is shown in (21), with $C(t)$ representing the time-of-use electricity price during the period t.

$$\min F = \sum P_{\text{grid}} \cdot \Delta t \cdot C(t) \tag{21}$$

The daily water demand of five crops at three locations are calculated for a 1000 m^2 greenhouse system by the crop evapotranspiration model proposed above, and the results are shown in Table III. The results indicate that evapotranspiration of crops in different places varies with geographical conditions.

TABLE III
THE IRRIGATION WATER DEMAND

Crop	Water demand (mm)		
	Chengdu	Haikou	Jinan
Lettuce	3.06806	3.83155	3.00727
Cabbage	2.95445	3.68964	2.89589
Tomato	3.40898	4.25727	3.34142
Sweet pepper	3.18172	3.97346	3.11866
Cucumber	3.06809	3.83155	3.00727

Haikou requires the largest water demand because of strong sunshine, low latitude and high average annual temperature, which accelerates the evapotranspiration of crops, followed by Chengdu. Owing to the high latitude and low altitude, the crops in Jinan require the least water for irrigation. The amount of water required for irrigation is expressed in millimeters. If the density of the water is 1000 kg/m^3, for example, around 3.068, 3.832, 3.007 t of water is needed for lettuce irrigation in a 1,000 m^2 (1.5 mu) greenhouse.

Based on (1), the daily lighting compensation of the five crops at different locations is shown in Table IV measured by hours. When estimating the amount of light compensation for tomato planting, it was found that the LED with 20 W could not provide sufficient light compensation to satisfy the photoperiod demand of the plant, so the power of the LED lamp was doubled, thus the load was doubled.

TABLE IV
THE LIGHT REQUIRED TO BE COMPENSATED

Crop	Lighting compensation (h)		
	Chengdu	Haikou	Jinan
Lettuce	4.1759	2.263	0.963
Cabbage	6.806	4.893	3.593
Tomato	8.3333	7.377	6.727
Sweet pepper	4.6296	2.717	1.417
Cucumber	6.9444	5.031	3.732

According to the calculated daily water demand and light compensation hours of crops, the cost-effective daily distribution of the irrigation water and lighting compensation for

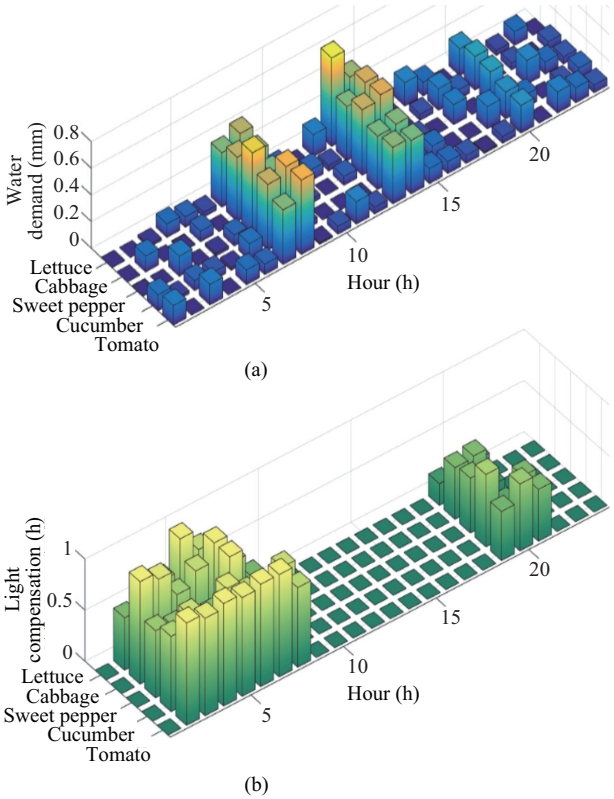

Fig. 4. Daily distribution of the required irrigation water and lighting compensation for five plants in Chengdu. (a) Water demand. (b) Light compensation.

five plants in Chengdu is shown in Fig. 4. These results are calculated by implementing the proposed optimization methods of the irrigation and light compensation systems.

The results illustrate that the irrigation system is primarily restricted by the irrigation regulation required by crop growth. The irrigation water is primarily concentrated at noon and morning to avoid crop water shortage caused by excessive evaporation. Irrigation is required less at night to reduce the potential waste of water. However, the irrigation system is less responsive to the electricity price as the main purpose of irrigation is to maintain the crop growth. In contrast, the behavior of the lighting compensation system will be changed due to the fluctuations of electricity price to save the electricity purchase cost from the grid, while still satisfying the essential constraints. As a result, the light system is primarily utilized at midnight when the electricity price is low and the natural sunshine is unavailable. However, there is also plenty of available lighting compensation achieved by the solar energy stored in the battery during the high price period of the evening.

Figure 5 shows that the load dispatch of both irrigation and light systems are responsive to the electricity price. In addition, the electricity consumption curve of the greenhouse is in accordance with the light compensation system load curve, indicating that the electricity consumption of the irrigation system is much less than that of the light compensation system. The light compensation system average power is 5,671.7 W, while the irrigation system average power is only 126 W. Therefore, the electricity consumption characteristics of the greenhouse are primarily determined by the light compensation system.

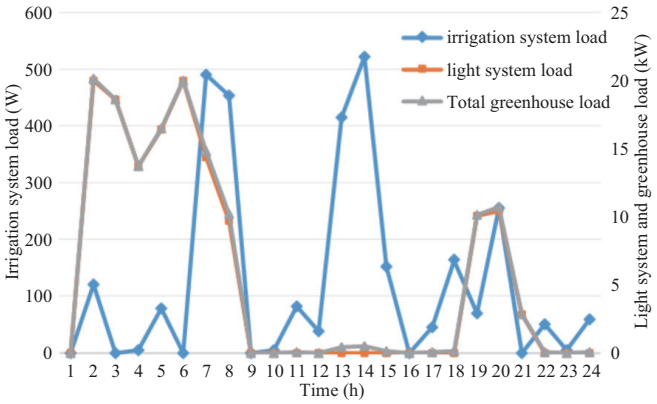

Fig. 5. Optimal greenhouse load curves in response to the electricity price.

The numerical data above describes the circumstances that crops are in the midseason of their growth period. When the crops are in a different growth period, the parameters vary in the model. In model (5), according to the definition of crop coefficient, the parameter K_c can effectively reflect the differences in the water demand of different plants in different growth cycles or different plants. In model (2), D_{target}, which represents the target light, will vary with crop type and growth period. Therefore, these two critical parameters of our agricultural load can be used to represent different growth stages and crop types, and the results are shown in Table V. The data indicates that in the midseason stage, more water and irrigation load are needed than in the initial stage or end season stage, because of the larger crop coefficient in the midseason. Also, the midseason growth stage of all crops requires the most illumination, so the light compensation load is highest when compared with the other stages. From the results, we can determine that the tomato is the most energy-intensive crop among these five crops, owing to the greater irrigation and light compensation requirements. In particular, lettuce being an end of season crop, requires less light, so it doesn't need light compensation. In order to further compare the advantages for the optimal operation of the agricultural load in a greenhouse system, a traditional power usage behavior is designed according to the traditional agricultural planting experience. The amount of irrigation water is shown in Table VI, while the lighting system continuously compensates illumination from 8 o'clock until the time of daily growth sunlight of the crop is satisfied.

TABLE VI
THE IRRIGATION WATER IN TRADITIONAL PLANTING MODE

City	Crop	Irrigation water volume (mm)		
		8:00 am	12:00 am	20:00 pm
Chengdu	Lettuce	0.7	1.8	0.6
	Cabbage	0.6	1.8	0.6
	Sweet pepper	0.7	1.9	0.6
	Cucumber	0.8	1.6	0.6
	Tomato	1	1.8	0.6
Haikou	Lettuce	1.3	2	0.5
	Cabbage	1.2	1.9	0.6
	Sweet pepper	1.3	2	0.6
	Cucumber	1.3	1.9	0.7
	Tomato	1.4	2.1	0.7
Jinan	Lettuce	1	1.5	0.5
	Cabbage	0.9	1.4	0.6
	Sweet pepper	1	1.6	0.6
	Cucumber	1	1.5	0.5
	Tomato	1.1	1.7	0.6

The cost comparison between the optimal operational mode and the traditional planting mode is shown in Table VII. According to the five different types of crops at three different

TABLE V
AGRICULTURAL LOAD IN DIFFERENT GROWTH PERIODS

Crop	Initial		Midseason		End season	
	Irrigation (W)/ K_c	Light compensation (kW) / Target DLI	Irrigation (W) / K_c	Light compensation (kW) / Target DLI	Irrigation (W) / K_c	Light compensation (kW) / Target DLI
Lettuce	1308.64/0.15	–/10.35	3132.00/0.95	83.52/14.51	2900.00/0.85	–/10.35
Cabbage	1308.64/0.15	88.52/14.78	3016.00/0.9	13.61/17.35	3016.00/0.9	88.52/14.78
Tomato	1308.64/0.15	25.93/24	3480.01/1.1	33.33/28	2668.00/0.75	25.93/24
Sweet pepper	1308.64/0.15	37.04/12	3248.00/1.0	92.59/15	2784.00/0.8	37.04/12
Cucumber	1308.64/0.15	37.04/12	3132.00/0.95	13.89/17.5	2552.00/0.7	37.04/12

TABLE VII
ELECTRICITY COST COMPARISON

City	Crop	Cost in optimal mode (yuan / d)	Cost in traditional mode (yuan / d)
Chengdu	Lettuce	26.818	40.984
	Cabbage	52.055	64.357
	Sweet pepper	32.101	45.182
	Cucumber	55.394	65.727
	Tomato	143.100	163.677
Haikou	Lettuce	12.575	19.399
	Cabbage	35.766	48.009
	Sweet pepper	16.629	25.115
	Cucumber	35.851	49.436
	Tomato	119.399	147.953
Jinan	Lettuce	1.328	5.519
	Cabbage	23.023	34.999
	Sweet pepper	5.101	8.707
	Cucumber	24.868	36.603
	Tomato	108.757	136.378

planting locations, the daily electricity cost savings is achieved in the range of 4.2–28.5 yuan per day, with the savings of the electricity proportion from 75.93% (the lettuce cultivation in Jinan) to 12.57% (the tomato planting in Chengdu). From the numerical data, tomato planting is high-cost in all locations, costing 143, 119, 108 yuan per day in optimal operational mode. The reason for that is because tomato growth requires more light compensation than other crops, which is shown in Table IV. That means tomato planting needs more power to satisfy its growth, which is not suitable for a power shortage area. On the contrary, lettuce is a low-cost type of crops, especially in a high latitude area. Compared with lettuce cultivation, tomato cultivation has a significant improvement in the cost of electricity, but its saving ratio is low, which is primarily caused by the wide variety of biomass demand of the crop itself. The results could provide a reference for suitable crop type selection at different cities for the economic operation of the greenhouse system considering the agricultural load modeling.

The purchased electricity from the grid is divided into three categories: plain electricity, peak electricity and valley electricity. The ratio of daily purchased power consumed by different crops at the greenhouse in either optimal operational mode or traditional operational mode are illustrated in Fig. 6, while Fig. 6(a) illustrates that in Chengdu, Fig. 6(b) and Fig. 6(c) indicates Jinan and Haikou respectively. The results show that crop planting uses more than 60% off-valley power in traditional customs. But after optimization, the working time of the artificial light shifts from peak periods to valley periods, which improves the power usage structure. In particular, for Chengdu, there is a distinct change in the electricity consumption structure of lettuce planting, which is 15.8% plain electricity and 84.2% peak electricity to 99.99% valley electricity and the trace of plain electricity and peak electricity, is shown in Fig. 6(a). Wherever the crop are planted, the electricity used in the growth process includes over 75% valley electricity after optimization. What is important is this electricity consumption structure is more amicable to the grid. Compared with the traditional operational mode, the optimal one could consume more power in valley periods and less power in peak periods, which is beneficial to absorb abandoned hydropower in the valley and reduce the peak and valley differences for smoothing the power system operation.

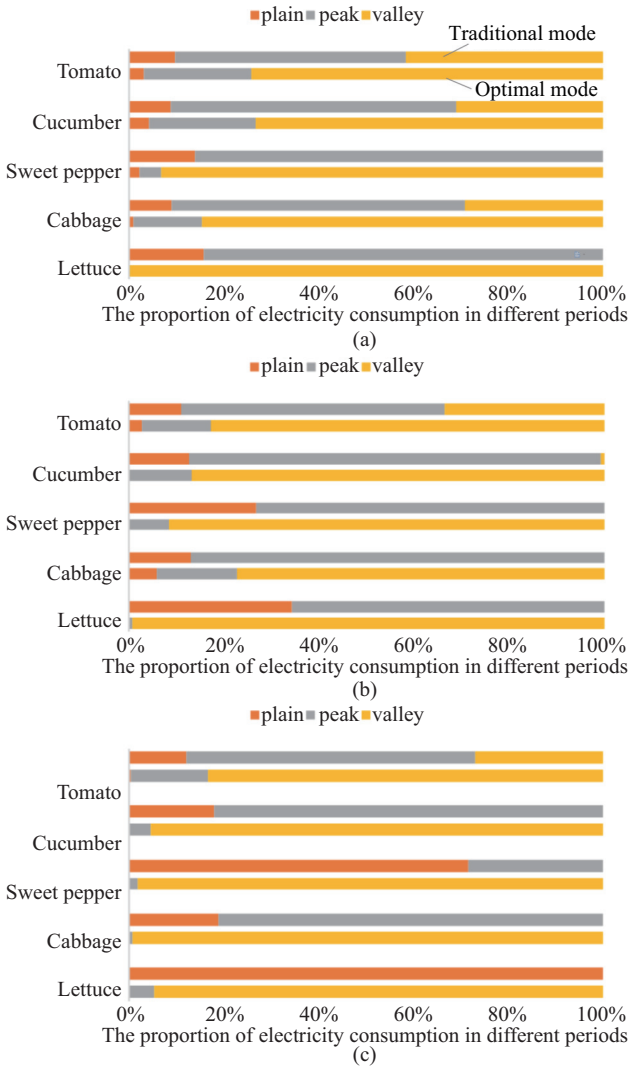

Fig. 6. Ratio of daily purchased power consumed by different crops in the greenhouse. (a) In Chengdu. (b) In Jinan. (c) In Haikou.

Further research announced by Li *et al.* indicated that the yield and market price of crops had a significant impact on the return of investment in greenhouses, based on the analysis of five PV greenhouses using the Annual Return on Investment (AROI) method [32], in order to provide a more comprehensive reference for the economic benefits of optimal greenhouse operations located in different cities. Factors including crop yield, growth cycle and wholesale market price have been taken into consideration. The information of yield, growth cycle and market price of each crop was collected from the China Agricultural Information Network [33], which is shown in the Table VIII.

The cultivation daily earnings in optimal greenhouse operations are shown in Fig. 7 and the economic improvement of crop planting in Chengdu, Jinan, and Haikou is shown in Fig. 8. As can be seen from Fig. 7, the tomato cultivation final earnings are greater than the other four crops because of its high yield and market price, although it has the highest daily electricity cost.Compared with the electricity cost shown in Table VI, after optimization, the influence of electricity cost of lettuce planting is the most positive, reduced by 75.93%

TABLE VIII
AGRICULTURAL INFORMATION OF CROPS

Crop	Yield (kg/m^2)	Life cycle (d)	Location	Market price (yuan/kg)
Lettuce	5.25	60	Chengdu	4.4
			Jinan	3.5
			Haikou	4
Cabbage	6.75	55	Chengdu	1.3
			Jinan	1.6
			Haikou	2.4
Sweet pepper	7.5	210	Chengdu	8.4
			Jinan	10.88
			Haikou	7.8
Cucumber	9	90	Chengdu	3.4
			Jinan	2.6
			Haikou	3.6
Tomato	30	150	Chengdu	5.6
			Jinan	7
			Haikou	5.2

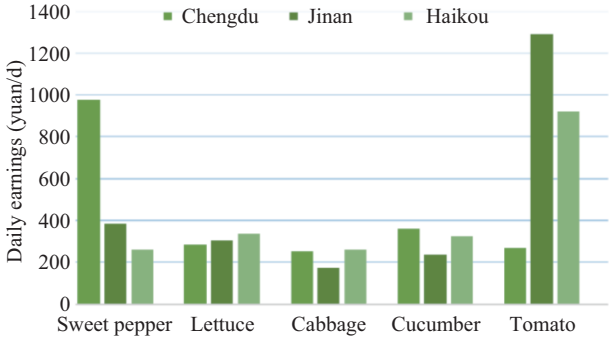

Fig. 7. Crop planting daily earnings in optimal operation.

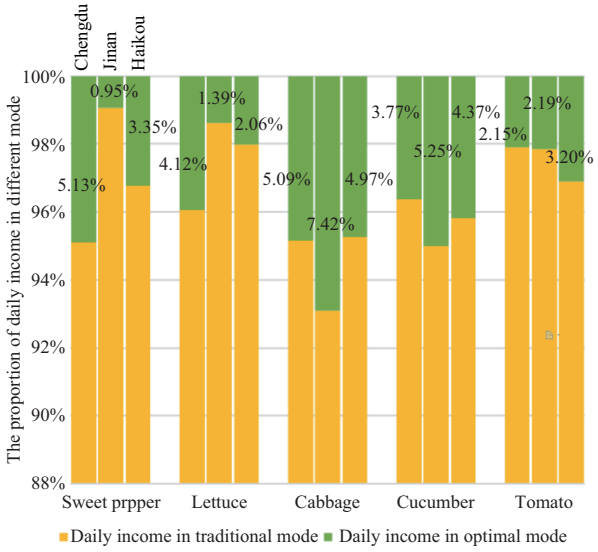

Fig. 8. Greenhouse economic improvement of crop planting (Daily income in optimal mode is 100%).

in Jinan, while the improvement of planting income is not obvious as expected, increasing by 4.12% in Chengdu, 1.39% in Jinan, and 2.06% in Haikou. The results indicate that for the same planting location, the planting economic improvement is affected by the crop types. In the Chengdu area, the most appreciable improvement is sweet pepper planting at 5.13%, while in the Jinan and Haikou areas, it is cabbage planting at 7.42% and 4.97% respectively. Because the tomato is a high yield type of crop, the highest-earnings will be obtained from tomato planting among these three areas.

IV. CONCLUSION

In this paper, a method of converting the crop growth mechanism into electricity consumption is proposed by considering the light and water requirements on crop growth in greenhouses. An agricultural load model is developed based on the crop evapotranspiration model and the daily light integral model. Power system simulation has been conducted to study the optimal operation of greenhouses with the proposed agricultural load model, PV generation and the battery energy storage system. Economic benefits from optimal operations of the greenhouse system are quantified. The following conclusions are drawn:

The load are primarily constituted by the artificial lighting compensation system. The irrigation system of the load is relatively negligible. The irrigation system primarily reduces the waste of water resources from irrigating soil to irrigating the crop. In addition, electricity consumption of the photovoltaic greenhouse can be optimized with maximum electricity cost savings of 75.93% under the proposed model. Furthermore, the overall income of agricultural production is improved by 7.43%.

The potential application of the model to guide the planning of rural distribution network construction, and the systematic approach to use the agricultural load for clean energy consumption will be investigated in a future work.

REFERENCES

[1] J. G. Liu, G. Q. Mao, A. Y. Hoekstra, H. Wang, J. H. Wang, C. M. Zheng, M. T.H. van Vliet, M. Wu, B. Ruddell, and J. Y. Yan, "Managing the energy-water-food nexus for sustainable development," *Applied Energy*, vol. 210, pp. 377–381, Jan. 2018.

[2] J. Y. Dai, S. Q. Wu, G. Y. Han, J. Weinberg, X. H. Xie, X. F. Wua, X. Q. Song, B. Y. Jia, W. Y. Xue, and Q. Q. Yang, "Water-energy nexus: A review of methods and tools for macro-assessment," *Applied Energy*, vol. 210, pp. 393–408, Jan. 2018.

[3] T. Y. Wang, G. X. Wu, J. W. Chen, P. Cui, Z. X. Chen, Y. Y. Yan, Y. Zhang, M. C. Lia, D. X. Niu, B. G. Li, and H. Y. Chen, "Integration of solar technology to modern greenhouse in China: Current status, challenges and prospect," *Renewable and Sustainable Energy Reviews*, vol. 70, pp. 1178–1188, Apr. 2017.

[4] J. Y. Liu, Y. X. Chai, Y. Xiang, X. Zhang, S. Gou, and Y. B. Liu, "Clean energy consumption of power systems towards smart agriculture: roadmap, bottlenecks and technologies," *CSEE Journal of Power and Energy Systems*, vol. 4, no. 3, pp. 273–282, Sep. 2018.

[5] Q. S. Xu, C. X. Yang, and Q. G. Yan, "Strategy of day-ahead power peak load shedding considering thermal equilibrium inertia of large-scale air conditioning loads," *Power System Technology*, vol. 40, no. 1, pp. 156–163, Jan. 2016.

[6] F. L. Quilumba, W. J. Lee, and J. Játiva-Ibarra, "Load models for flat-panel TVs," *IEEE Transactions on Industry Applications*, vol. 50, no. 6, pp. 4171–4178, Mar./Dec. 2014.

[7] K. McKenna and A. Keane, "Open and closed-loop residential load models for assessment of conservation voltage reduction," *IEEE Transactions on Power Systems*, vol. 32, no. 4, pp. 2995–3005, Jul. 2017.

[8] L. D. Wang, W. He, and Z. L. Piao, "Voltage step point detection and parameter identification of general dynamic load model," *Power System Technology*, vol. 38, no. 9, pp. 2479–2483, Sep. 2014.

[9] X. Qu, X. R. Li, J. Y. Song, and C. He, "An extended composite load model taking account of distribution network", *IEEE Transactions on Power Systems*, vol. 33, no. 6, pp. 7317–7320, Nov. 2018.

[10] J. V. Milanovic, K. Yamashita, S. M. Villanueva, S. Ž. Djokic, and L. M. Korunović, "International industry practice on power system load modeling," *IEEE Transactions on Power Systems*, vol. 28, no. 3, pp. 3038–3046, Aug. 2013.

[11] Y. L. Zhao and Y. Gao, "The loadforecasting of rural power system—based on excel regression model," *Journal of Agricultural Mechanization Research*, no. 2, pp. 226–228, 244, Feb. 2014.
[12] Q. H. Lai, B. L. Mi, and Z. J. Yang, "Forecasting of agricultural machine power of Heilongjiang province based on artificial nerve network model," *Journal of Agricultural Mechanization Research*, no. 4, pp. 272–274, Jul. 2005.
[13] R. F. Guo, W. J. Li, X. R. Wang, B. X. Chen, Z. K. Huang, T. Liu, X. D. Chen, X. X. Han, and Z. X. Lai, "Effect of photoperiod on the formation of cherry radish root," *Scientia Horticulturae*, vol. 244, pp. 193–199, Jan. 2019.
[14] M. Nico, D. J. Miralles, and A. G. Kantolic, "Natural post-flowering photoperiod and photoperiod sensitivity: Roles in yield-determining processes in soybean," *Field Crops Research*, vol. 231, pp. 141–152, Feb. 2019.
[15] Z. N. Yan, D. X. He, G. H. Niu, and H. Zhai, "Evaluation of growth and quality of hydroponic lettuce at harvest as affected by the light intensity, photoperiod and light quality at seedling stage," *Scientia Horticulturae*, vol. 248, pp. 138–144, Apr. 2019.
[16] Y. P. Sun, Y. B. Sun, Z. C. Sun, Q. Liu, P. W. Li, and C. Z. Li, "Mapping monthly distribution of daily light integrals across China," *Hunan Forestry Science & Technology*, vol. 42, no. 4, pp. 43–47, Aug. 2015.
[17] X. Zhang, "Technical foundation of environmental feedback control of hydroponic lettuce based on photosynthesis simulation," Ph.D. dissertation, China Agricultural University, Beijing, China, 2017.
[18] X. P. Song, H. T. W. Tan, and P. Y. Tan, "Assessment of light adequacy for vertical farming in a tropical city," *Urban Forestry & Urban Greening*, vol. 29, pp. 49–57, Jan. 2018.
[19] R. C. Morrow, "LED lighting in horticulture," *HortScience*, vol. 43, no. 7, pp. 1947–1950, Dec. 2008.
[20] R. H. E. Hassanien, M. Li, and W. D. Lin, "Advanced applications of solar energy in agricultural greenhouses," *Renewable and Sustainable Energy Reviews*, vol. 54, pp. 989–1001, Feb. 2016.
[21] Y. Q. Xu, "Optimal design of LED assembled light source & its application in greenhouse plant production," M.S. thesis, Department of Biophysics, Zhejiang A&F University, Hangzhou, China, 2017.
[22] Z. S. Wang, "Optimization of winter wheat irrigation schedule in Guangzhong region Shaanxi province by crop models," M.S. thesis, Department of Agricultural Soil and Water Engineering, Northwest A&F University, Xianyang, China, 2016.
[23] X. J. Li, S. Z. Kang, J. Niu, Z. L. Huo, and J. Z. Liu, "Improving the representation of stomatal responses to CO_2 within the Penman–Monteith model to better estimate evapotranspiration responses to climate change," *Journal of Hydrology*, vol. 572, pp. 692–705, May 2019.
[24] A. Ershadi, M. F. McCabe, J. P. Evans, and E. F. Wood, "Impact of model structure and parameterization on Penman-Monteith type evaporation models," *Journal of Hydrology*, vol. 525, pp. 521–535, Jun. 2015.
[25] M. M. Davis and S. Hirmer, "The potential for vertical gardens as evaporative coolers: An adaptation of the 'Penman Monteith Equation'," *Building and Environment*, vol. 92, pp. 135–141, Oct. 2015.
[26] J. D. Valiantzas, "Simplified forms for the standardized FAO-56 Penman-Monteith reference evapotranspiration using limited weather data," *Journal of Hydrology*, vol. 505, pp. 13–23, Nov. 2013.
[27] L. Olivera-Guerra, O. Merlin, S. Er-Raki, S. Khabba, and M. J. Escorihuela, "Estimating the water budget components of irrigated crops: Combining the FAO-56 dual crop coefficient with surface temperature and vegetation index data," *Agricultural Water Management*, vol. 208, pp. 120–131, Sep. 2018.
[28] Y. Yang, Y. L. Cui, K. H. Bai, T. Y. Luo, J. F. Dai, W. G. Wang, and Y. F. Luo, "Short-term forecasting of daily reference evapotranspiration using the reduced-set Penman-Monteith model and public weather forecasts," *Agricultural Water Management*, vol. 211, pp. 70–80, Jan. 2019.
[29] V. Phogat, J. Šimůnek, M. A. Skewes, J. W. Cox, and M. G. McCarthy, "Improving the estimation of evaporation by the FAO-56 dual crop coefficient approach under subsurface drip irrigation," *Agricultural Water Management*, vol. 178, pp. 189–200, Dec. 2016.
[30] S. Irmak, T. A. Howell, R. G. Allen, J. O. Payero, and D. L. Martin, "Standardized ASCE Penman-Monteith: Impact of sum-of-hourly vs. 24-hour timestep computations at reference weather station sites," *Transactions of the ASAE*, vol. 48, no. 3, pp. 1063–1077, May 2005.
[31] J. Carroquino, R. Dufo-López, and J. L. Bernal-Agustín, "Sizing of off-grid renewable energy systems for drip irrigation in Mediterranean crops," *Renewable Energy*, vol. 76, pp. 566–574, Apr. 2015.
[32] C. S. Li, H. Y. Wang, H. Miao, and B. Ye, "The economic and social performance of integrated photovoltaic and agricultural greenhouses systems: Case study in China," *Applied Energy*, vol. 190, pp. 204–212, Mar. 2017.
[33] China Agricultural Information Network, [Online]. Available: http://www.agri.cn/, Jan. 2019.

Zeming Li received the B.S. degree in Electrical Engineering and Automation from Sichuan University in 2018. He is currently pursuing his M.S. degree in Power System and Automation in Sichuan University, Chengdu, China. His research interests include agricultural load and distributed energy consumption.

Junyong Liu (M'17) received the Ph.D. degree in Electrical Engineering from Brunel University, UK, in 1998. He is a Professor in the College of Electrical Engineering and Information Technology, Sichuan University, China. His main research interests are power market, power system planning, operations, and stability and computer applications.

Yue Xiang (SM'21) received the B.S. and Ph.D. degrees in Electrical Engineering from Sichuan University, China, in 2010 and 2016, respectively. From 2013 to 2014, he was a joint Ph.D. student at the Department of Electrical Engineering and Computer Science, University of Tennessee, Knoxville, USA and also a visiting scholar at the Department of Electronic and Electrical Engineering, University of Bath, UK in 2015. He is currently an Associate Professor in the College of Electrical Engineering and Information Technology, Sichuan University, China. His main research interests are power system planning and optimal operations, renewable energy integration and smart grids.

Xin Zhang (SM'20) received the B.Eng. degree in Automation from Shandong University, China, in 2006; his M.Sc. and Ph.D. degrees in Electrical Power Engineering from The University of Manchester, U.K., in 2007 and 2010 respectively. He is a Senior Lecturer (Associate Professor) in energy systems at Cranfield University, U.K. His recent research activities include sustainable energy systems for the electrification of airports and aviation. From 2011 to 2019, he was a Power System Engineer at the National Grid U.K., where he took various roles including national energy strategy, power system analysis and power market operations, primarily in the GB Electricity National Control Center. His research interests include power system planning and operations, smart energy networks with the integration of renewable and multi-vector energy sources. He is a Chartered Engineer with the U.K. Engineering Council.

Yanxin Chai received the B.Eng. degree in Electrical Engineering and Automation from Sichuan University, China, in 2017. She is now studying for her M.Sc. degree in Electrical Engineering from Sichuan University, China. Her research interests include investment and planning of distribution networks.